Published in final edited form as:
Microfluid Nanofluidics. 2010 February 1; 8(2): 263–268. doi:10.1007/s10404-009-0503-9.

Single cell trapping in larger microwells capable of supporting cell spreading and proliferation

Joong Yull Park[1], **Mina Morgan**[1], **Aaron N. Sachs**[1], **Julia Samorezov**[1], **Ryan Teller**[1], **Ye Shen**[1], **Kenneth J. Pienta**[2], and **Shuichi Takayama**[1]

Shuichi Takayama: takayama@umich.edu

[1] Department of Biomedical Engineering, College of Engineering, University of Michigan, 2200 Bonisteel Blvd, Ann Arbor, MI 48109, USA

[2] Departments of Internal Medicine and Urology, Michigan Center for Translational Pathology and the Comprehensive Cancer Center, University of Michigan, 1500 E. Medical Center Drive, Ann Arbor, MI 48109, USA

Abstract

Conventional cell trapping methods using microwells with small dimensions (10–20 μm) are useful for examining the instantaneous cell response to reagents; however, such wells have insufficient space for longer duration screening tests that require observation of cell attachment and division. Here we describe a flow method that enables single cell trapping in microwells with dimensions of 50 μm, a size sufficient to allow attachment and division of captured cells. Among various geometries tested, triangular microwells were found to be most efficient for single cell trapping while providing ample space for cells to grow and spread. An important trapping mechanism is the formation of fluid streamlines inside, rather than over, the microwells. A strong flow recirculation occurs in the triangular microwell so that it efficiently catches cells. Once a cell is captured, the cell presence in the microwell changes the flow pattern, thereby preventing trapping of other cells. About 62% of microwells were filled with single cells after a 20 min loading procedure. Human prostate cancer cells (PC3) were used for validation of our system.

Keywords

Single cell trapping; Microwell; Recirculation; Continuous flow

1 Introduction

Microwells are frequently used in biology and tissue engineering research such as embryoid body formation (Mohr et al. 2006; Karp et al. 2007; Moeller et al. 2008), multicellular organization (Ungrin et al. 2008), and three-dimensional (3D) tissue cultivation (Gottwald et al. 2007). However, many of these research applications allow (or must achieve) trapping of multiple cells in each microwell. Single cell trapping is necessary to allow identification of differing cell phenotypes within a population of cells (Di Carlo and Lee 2006). Single cell manipulation using microwells also enables observation of the direct descendants of single cells cultured under controlled biological conditions (Inoue et al. 2001), the analysis of intracellular compounds (Chao and Ros 2008), and the measurement of electrical functionality

Correspondence to: Shuichi Takayama, takayama@umich.edu.

Electronic supplementary material The online version of this article (doi:10.1007/s10404-009-0503-9) contains supplementary material, which is available to authorized users.

of cells (Moss et al. 2007). The above reports, however, are limited in throughput, mainly because of the difficulty in achieving high-throughput single cell trapping, and also because of the innate limitations in imaging capacity.

Therefore, there is a need for development of tools for high-throughput single cell trapping, culture, and analysis. Folch's group has developed a large-scale single-cell trapper using microwell arrays (Rettig and Folch 2005). They fabricated microwell arrays with microwell diameters of 20–40 μm, and correlated the microwell size with cell trapping rate, showing that the single cell trapping rate drops rapidly when the microwell size becomes larger (30–40 μm) than the single cell size (10–20 μm). Another outstanding report was made by Lee's group (Di Carlo et al. 2006) where U-shaped microstructures were utilized to trap single cells. However, these two systems provide only limited room for cell growth and division or allow only limited cell motion/activity (though one should note that the systems are very good for short-term culture or observing instantaneous response of cells). Also, the fabrication process for these systems requires high-end facilities with single-digit micron scale resolution of features. Takeuchi's group proposed a robust system for trapping and releasing cells in a series of micropockets using a unique feature of hydrodynamic confinement (Tan and Takeuchi 2007); however, the lack of space for cell growth and division was yet unsolved. Rosenthal and Voldman (2005) proposed another trapping method that provides space for cell growth by using dielectrophoresis for single cell patterning on 5 × 5 arrayed electrodes, but the need of electrode patterning and circuit control is complicating.

Here, we report a method for high-throughput single cell trapping in larger, more readily fabricated microwells by utilizing slow laminar flow and optimized microwell shape to achieve high cell-entrapment rates (Fig. 1a). Two requirements were set for the test of this method: (1) cmicrowells should trap single cells and (2) the size of microwells should be 50 μm or larger to provide enough room for cell growth and division as well as to simplify fabrication. We note that microwells with dimensions of 50 μm will typically trap multiple cells in each microwell if no other mechanism prevents this (Rettig and Folch 2005). Previously, the Khademhosseini group cleverly showed that trapping of multiple cells can be achieved by microcirculation of flow within long parallel microchannels (Manbachi et al. 2008); they used experimental methods and computational simulations to optimize trapping of multiple cells in long microscale grooves useful for cell alignment. In this article, we investigate more closely how geometry of microwells affects the flow pattern and ability of microwells to trap single cells. The overall system geometry in Fig. 1b shows the two components of the device—the microwell array and the main channel. The microwell array had a typical well side length and spacing of 50 μm, and depth of 20 μm, providing ~10,000 total microwells in a channel. The main channel measures 200 μm, 5 mm, and 15 mm in height, width, and length, respectively; it fits over the microwell array to allow cell solution flow across the array. Prostate cancer cells were used for validation of this method. Even though we specify one microwell dimension in detail in this article, the logic introduced in this article will be applicable to different microwell sizes and different types of cells.

2 Materials and methods

2.1 System design

The system consists of a microwell array that covers the bottom of the chip, and a long narrow channel (5 mm width, 15 mm length, and 200 μm height) that guides fluid flow over it. A 50 × 200 array of triangular microwells (typical side length dimension of 50 μm with depth of 20 μm) extends downward into the bottom layer giving a total of 10,000 microwells. At the inlet of this chip, a reservoir (diameter of 5 mm, height of 5 mm, and total volume of about 100 μl) was equipped, and at the outlet (see Fig. 1b), a syringe pump (KDS 210 Syringe Pump; KD Scientific, Holliston, MA), loaded with a 1 ml syringe, pulls the fluid to generate flow rates

varying from 0.05 to 0.18 ml/h (average velocity in channel = 14–50 μm/s). The cell suspension enters the microchip, flows through the channel, and cells settle into the microwells. Cell perfusion times were limited to 20 min. To prevent the cells from settling down onto the bottom of inlet reservoir, we intentionally mixed the cell suspension in the inlet reservoir using pipette at about 1 min intervals.

2.2 Computational evaluation of microwell designs

Simulations were performed to observe the effect of streamlines generated near individual microwells for trapping cells. 3D simulations were generated using a commercial program, FLUENT 6.3 (Fluent Inc., Canonsburg, PA) for five different shapes of microwell: triangle, square, circle, diamond, and cone shape (see Fig. 1c). The working fluid was assumed to be water (a homogeneous, incompressible, Newtonian fluid; density 998.2 kg/m^3, dynamic viscosity 0.001 kg/m s), and the flow was assumed to be laminar and steady. The Navier–Stokes equations and the conservation equation were calculated. For boundary conditions, a periodic condition was used for inlet/outlet faces (the flow profile calculated at the outlet face of computational domain is to be used for the inlet flow profile, iteratively), a symmetric condition for the side faces, and a no slip condition for the top and bottom of the channel (Fig. 2a). Use of periodic and symmetric conditions reduced the required computing power greatly without losing accuracy in computational result. The flow velocity of 100 μm/s was applied. Convergence was regarded as having been achieved when residuals of momentum and conservation equations reached 10^{-6}.

2.3 Cell culture

Human PC3 prostate cancer cells originally isolated from vertebral metastases in a prostate cancer patient was obtained from ATCC (Rockville, MD). PC3 cells were cultured in T-25 flasks (Corning, Acton, MA) and maintained in complete media consisting of RPMI-1640 (61870; Gibco, Carlsbad, CA) supplemented with 10% (v/v) fetal bovine serum (FBS; 10082; Gibco), and 1% (v/v) penicillin–streptomycin (Invitrogen, Carlsbad, CA). All cultures were maintained in a humidified incubator at 37°C, 5% CO_2, and 95% humidity. The prepared cells were then loaded into the device at the density of 1.5×10^6 cells/ml. To show cell spreading and proliferation, fluorescent images were taken by using an inverted fluoresence microscope (Eclipse TE300; Nikon, Tokyo, Japan).

3 Results and discussion

3.1 Microwell shape analysis

As a typical cell flows through a microchannel, it will gradually settle toward the bottom surface due to gravity (Fig. 1a). Generally, cells are 2–5% heavier than culture medium (although there are exceptions such as adipocytes) (Wolff and Pertoft 1972;Park et al. 2008). As the cell nears the bottom surface, it follows streamlines leading into the microwells while losing velocity. Depending on the velocity of the cell and its position relative to the micro-wells, a cell may approach a threshold slow speed at which point gravity shifts the cell into a lower streamline that leads into a recirculation zone in the microwell. Recirculation is a unique flow phenomenon that effectively captures and traps particles in this zone. Among the five different microwell geometries listed in Fig. 1c (equilateral triangle, square, circle, rhombus, and cone), we determined the equilateral triangle to be the best well shape because it had the strongest recirculation pattern in the microwell from 3D simulations (Fig. 2b). The rest of the shapes (square, circle, rhombus, and cone) had smaller recirculation zones in the corners of the wells. For the triangular geometry, we tested the effect of recirculation of the flow by using commercial latex beads (1.5×10^6 beads/ml, diameter 10 μm; Beckman Coulter, Fullerton, CA); the trapped beads at the downstream part of the triangular microwells moved slowly to the upstream corner (Fig. 2c), and this proved the existence of recirculation flow, helping to

trap cells as illustrated in Figs. 1a and 2b. However, cells are sticker than beads and thus some cells did not show such movements in our experiments.

The triangular geometry has another advantage for single cell trapping in that it can be easily scaled to accommodate variations in target cell size. The sample cell type used for our study was prostate cancer cells, with a typical size distribution of 20 ± 3.4 μm (manually measured). Typically, single cell filling of microwells is accomplished by using small wells. By using a combination of triangular wells and laminar flow, however, we can take advantage of cell trapping mediated streamline profile changes to prevent other cells from being trapped in the same microwell. As illustrated in Fig. 2d, triangular wells are advantageous for single cell trapping as compared to square and circular microwells because cells crossing the edge of the triangle microwell will not encounter any strong recirculation of streamlines. This means that only cells crossing the center will be trapped, limiting multiple cell trapping.

Our device does not kill or damage the cells during the trapping process. It has been shown experimentally that at shear stresses above 0.5 Pa, cells start to die, and at shear stresses above 0.2 Pa, cells experience phenotypical changes (Manbachi et al. 2008). In our 3D microwell simulations, an average velocity of 100 μm/s was chosen for an appropriate starting point for trapping considering two main parameters: maximum shear stress at the channel walls, and the pattern of the streamlines in the wells. However, we ran simulations with the triangle geometry at three different fluid velocities: 10, 100, and 1,000 μm/s. At 10 and 1,000 μm/s compared to the 100 μm/s average fluid velocities, the streamline pattern is slightly raised, implying that the fluid passes over instead of into the wells (see Fig. S1 in Supplementary Information). This indicates that the velocity in this range of magnitude does not change the streamline pattern. At 1,000 μm/s the maximum shear stress occurring at the channel walls is 0.2 Pa, which is approaching our design limit; at 0.2 Pa we cannot be positive that the cell phenotype will not be altered. The combination of a strong, low recirculation pattern and a safe 0.02 Pa maximum shear stress led us to choose 100 μm/s as a starting point for our average fluid velocity. However, experimentation led us to find an average fluid velocity range of 14–50 μm/s is best for cell trapping; this range of velocity was safe from harmful shear stress effect and also allowed cells to be dragged downward into the microwells. In our system cells attached on the channel floor (not in the microwell) would experience shear stress (τ) as follows. Here, the cell shape is simplified to be a hemisphere (Gaver and Kute 1998; Manbachi et al. 2008; Farokhzad et al. 2005).

$$\tau_{\max-\text{cell}} = 2.95\tau_{\text{free}-\text{cell}} = 2.95\,(6\mu Q/H^2 W) \tag{1}$$

where μ is the viscosity of water (0.001 Pa s), Q is the flow rate, H is the height of the channel (200 μm), and W is the width (5 mm). The calculated shear stress from Eq. 1, according to the level of flow rate used in our device, is 0.001 Pa for 0.05 ml/h (14 μm/s) and 0.004 Pa for 0.18 ml/h (50 μm/s).

3.2 Quantification of cell trapping rate

Our system design utilizes a syringe pump to generate flow of a cell suspension, captures cells in a microarray (10,000 microwells) using the principle of recirculation in micro-wells, and eliminates excess media using a second rinsing step. A long main channel (15 × 5 mm) was appropriate because it increased the possibility of trapping due to longer residence time. Validation of the trapping rate was conducted using PC3 cells. With the PC3 cells at a cell solution density of 1.5×10^6 cells/ml, a trial was conducted using a step-down flow rate sequence; initially 0.18 ml/h for 5 min to fill the channel with cells, and then 0.1 ml/h (for better results we controlled the flow rate in a range of 0.05–0.15 ml/h) for cell trapping for 10

min, followed by washing out 0.18 ml/h for 5 min. The total experiment time was 20 min. The typical cell trapping images are as shown in Fig. 3a. The trapping rate was 62 ± 10%, with a minimum rate of 48% and a maximum rate of 79%. Trapping rates were determined from three experiments. In each experiment, images (~100 micro-wells in each image) were taken at three random locations in the microchannels (see Fig. 3b). Among the microwells with cells, 5.7% were occupied by two cells and less than 0.2% were occupied by three cells. One may extend the duration of cell flow to increase trapping rate; however, it should be noted that the probability of trapping cells in a new empty microwell decreases as they are filled with cells. For example, the first cell entering the channel has the highest probability to be trapped because all microwells are vacant, and the last cell has a very limited chance to be trapped because many microwells are already filled. It was also observed that lower flow velocities slightly increased the trapping rate but also increased the likelihood of multiple-cell trapping. Overall trapping rate was more strongly dependent on cell density in suspension and duration of operation. In addition, it should be noticed that the recirculating streamline profile in the microwell does not change according to the flow rates (Fig. S1, Supplementary Information), implying same efficacy for trapping cells in different flow velocities.

The system design is such that after a cell suspension is flown across the microarray, the user can easily flush the system with either cell culture media or a phosphate buffer saline (PBS) at 0.18 ml/h to remove excess cells. This is fast enough to wash away untrapped cells, but slow enough to not dislodge trapped cells. In addition, the unique feature of the flowing method, which continuously washes away cells in the channel, effectively prevented a channel-blocking problem which can easily happen by cell gathering and sticking onto substrates in static conditions.

In summary, our system design utilizes continuous flow to deliver a cell suspension to the microarray and captures single cells via recirculation in each triangular well. Single cell trapping was successful even using large size micro-wells because the trapping of cells is controlled by fluid dynamics and assisted by the triangular geometry of each microwell. Current testing indicated a cell-trapping rate of 62 ± 10% with PC3 cells. The main limitations of our system are that trapping rate cannot exceed 60–70% in 20 min due to the settling probability, that a cover is required to create the channel, restricting access to the microwells during cell seeding and that a pump is necessary. However, our method has the advantage that many pre-reported microfluidic systems which utilize microfluidic networks can be conveniently applied to our system and that cell culture is possible due to the ample space of the microwells (Fig. 3c) allowing investigation of both long-term cell responses and instantaneous cell reactions. The methodology introduced in this article will lead to an effective and high-throughput cell-trapping device for screening that requires single cell capture and culture.

Supplementary Material

Refer to Web version on PubMed Central for supplementary material.

Acknowledgments

The authors would like to thank Chentian Zhang for assisting experiments, and Dr. Rachel Schmedlen for supporting a student team consisting of five authors who contributed equally to this study: M. Morgan, A. N. Sachs, J. Samorezov, R. Teller, and Y. Shen. This study was supported by the Wilson Foundation, Coulter Foundation, and the UMCCC Prostate SPORE P50 CA69568 pilot grant. Dr. J. Y. Park was supported by the Korea Research Foundation Grant, Republic of Korea (KRF-2008-357-D00030). Dr. K. J. Pienta is supported by NIH Grant PO1 CA093900, an American Cancer Society Clinical Research Professorship, NIH SPORE in prostate cancer Grant P50 CA69568, and the Cancer Center support Grant P30 CA46592. This work was supported in part by a generous grant from Mr. and Mrs. Turner.

References

Chao TC, Ros A. Microfluidic single-cell analysis of intracellular compounds. J R Soc Interface 2008;5 (Suppl 2):S139–S150. [PubMed: 18682362]

Di Carlo D, Lee LP. Dynamic single-cell analysis for quantitative biology. Anal Chem 2006;78:7918–7925. [PubMed: 17186633]

Di Carlo D, Wu LY, Lee LP. Dynamic single cell culture array. Lab Chip 2006;6:1445–1449. [PubMed: 17066168]

Farokhzad OC, Khademhosseini A, Jon S, Hermmann A, Cheng J, Chin C, Kiselyuk A, Teply B, Eng G, Langer R. Microfluidic system for studying the interaction of nanoparticles and microparticles with cells. Anal Chem 2005;77:5453–5459. [PubMed: 16131052]

Gaver DP III, Kute SM. A theoretical model study of the influence of fluid stresses on a cell adhering to a microchannel wall. Biophys J 1998;75:721–733. [PubMed: 9675174]

Gottwald E, Giselbrecht S, Augspurger C, Lahni B, Dambrowsky N, Truckenmuller R, Piotter V, Gietzelt T, Wendt O, Pfleging W, Welle A, Rolletschek A, Wobus AM, Weibezahn KF. A chip-based platform for the in vitro generation of tissues in three-dimensional organization. Lab Chip 2007;7:777–785. [PubMed: 17538721]

Inoue I, Wakamoto Y, Moriguchi H, Okano K, Yasuda K. On-chip culture system for observation of isolated individual cells. Lab Chip 2001;1:50–55. [PubMed: 15100889]

Karp JM, Yeh J, Eng G, Fukuda J, Blumling J, Suh KY, Cheng J, Mahdavi A, Borenstein J, Langer R, Khademhosseini A. Controlling size, shape and homogeneity of embryoid bodies using poly(ethylene glycol) microwells. Lab Chip 2007;7:786–794. [PubMed: 17538722]

Manbachi A, Shrivastava S, Cioffi M, Chung BG, Moretti M, Demirci U, Yliperttula M, Khademhosseini A. Microcirculation within grooved substrates regulates cell positioning and cell docking inside microfluidic channels. Lab Chip 2008;8:747–754. [PubMed: 18432345]

Moeller HC, Mian MK, Shrivastava S, Chung BG, Khademhosseini A. A microwell array system for stem cell culture. Biomaterials 2008;29:752–763. [PubMed: 18001830]

Mohr JC, de Pablo JJ, Palecek SP. 3-D microwell culture of human embryonic stem cells. Biomaterials 2006;27:6032–6042. [PubMed: 16884768]

Moss ED, Han A, Frazier AB. A fabrication technology for multi-layer polymer-based microsystems with integrated fluidic and electrical functionality. Sensors Actuat B 2007;121:689–697.

Park K, Jang J, Irimia D, Sturgis J, Lee J, Robinson JP, Toner M, Bashir R. 'Living cantilever arrays' for characterization of mass of single live cells in fluids. Lab Chip 2008;8:1034–1041. [PubMed: 18584076]

Rettig JR, Folch A. Large-scale single-cell trapping and imaging using microwell arrays. Anal Chem 2005;77:5628–5634. [PubMed: 16131075]

Rosenthal A, Voldman J. Dielectrophoretic traps for single-particle patterning. Biophys J 2005;88:2193–2205. [PubMed: 15613624]

Tan WH, Takeuchi S. A trap-and-release integrated microfluidic system for dynamic microarray applications. Proc Natl Acad Sci USA 2007;104:1146–1151. [PubMed: 17227861]

Ungrin MD, Joshi C, Nica A, Bauwens C, Zandstra PW. Reproducible, ultra high-throughput formation of multicellular organization from single cell suspension-derived human embryonic stem cell aggregates. PLoS ONE 2008;3:e1565. [PubMed: 18270562]

Wolff DA, Pertoft H. Separation of HeLa cells by colloidal silica density gradient centrifugation. I. Separation and partial synchrony of mitotic cells. J Cell Biol 1972;55:579–585. [PubMed: 4571230]

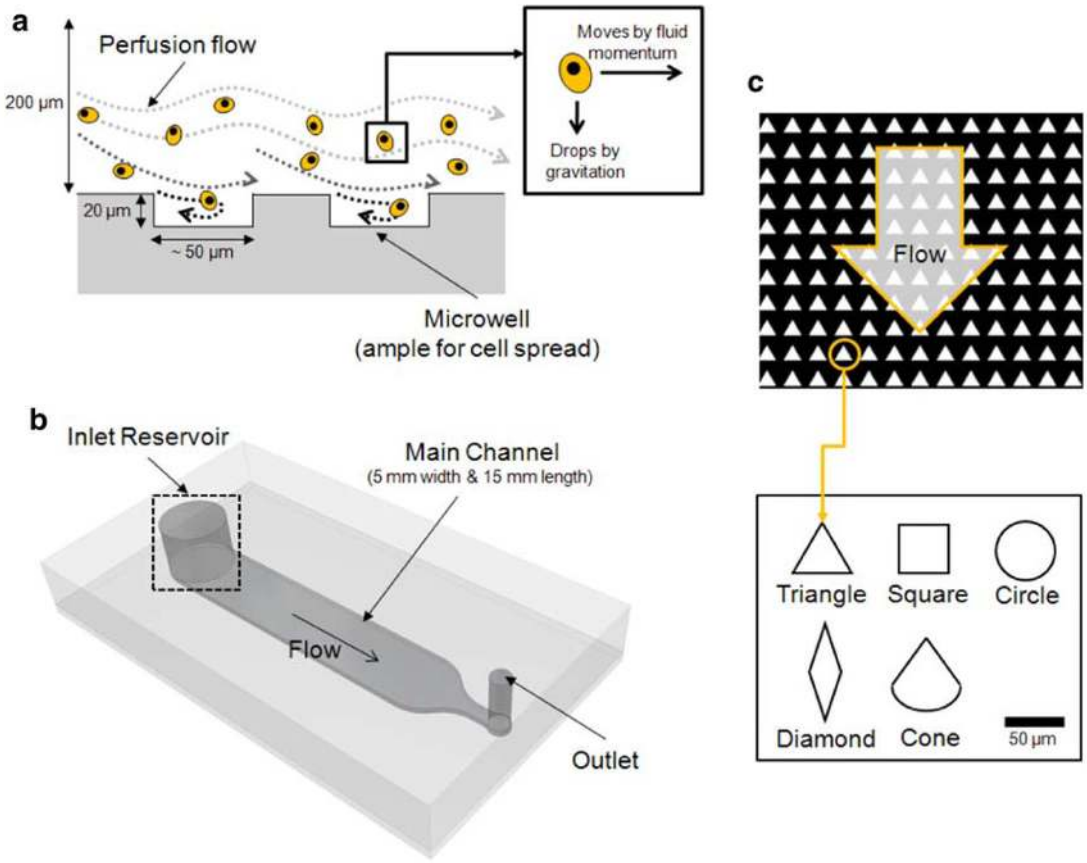

Fig. 1.

a During the perfusion of cell suspension in the channel, the cells sink gradually due to gravity, and some cells are caught in microwells while others pass and are carried away by flow. The in-well recirculating flow patterns can trap cells effectively. **b** The system consists of four parts: inlet reservoir where the cell suspension is introduced, main channel, microwells (not shown in the figure) patterned on the bottom surface of the main channel, and the outlet which is connected to a pulling syringe pump. Cell settling in the inlet reservoir was prevented by frequent pipettings. **c** Five different shapes of microwell were tested in simulations. The flow direction and the microwell geometry are aligned in the directions shown in this figure. Scale bar is 50 μm

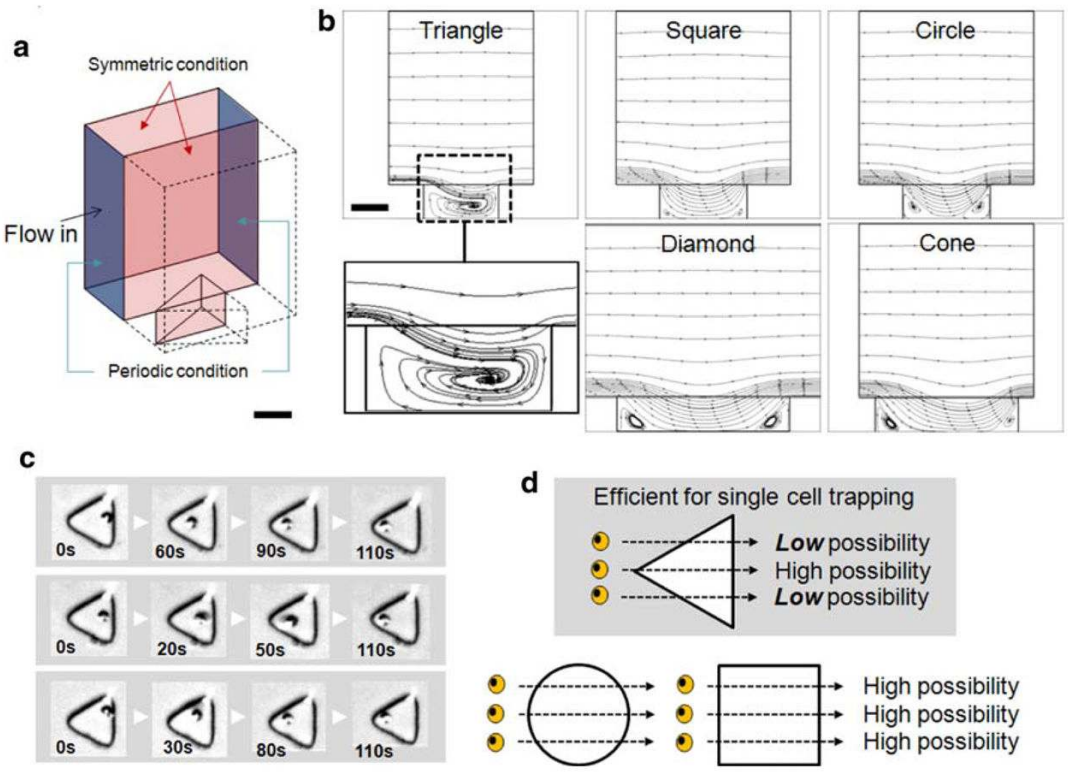

Fig. 2.

a A simple computational domain was constructed by applying a periodic condition and a symmetric condition. Scale bar is 20 μm. **b** Flow field visualized by streamlines in each microwell model shows that the triangular microwell has the most efficient profile (strong recirculation) of streamlines for trapping of a cell. Streamlines of each model are in same intensity. Scale bar is 20 μm. **c** Due to recirculation of flow in the microwell, trapped beads (diameter 10 μm) move slowly to the upper corner of the triangular microwells. **d** Geometry of microwell affects the trapping rate. There are more possibilities for trapping multiple cells in circular and square microwells because when cells travel over any regions of circular or square wells they travel the nearly same distance over the well, providing about equal chances of being trapped anywhere. On the contrary, the triangular well provides different trapping possibilities when the cell travels through the middle path and side paths

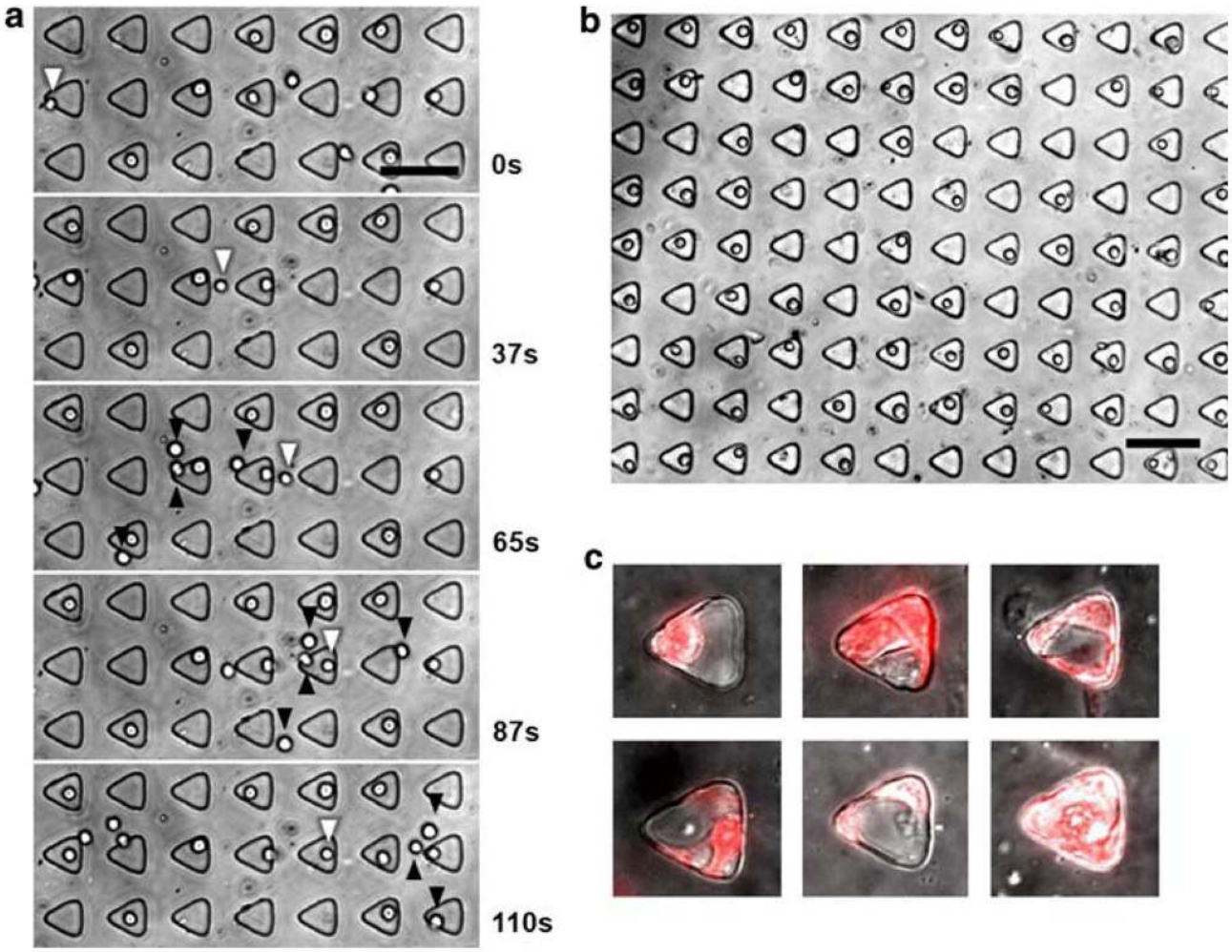

Fig. 3.

a Time lapse images of a trapping cell (*white arrowhead*). A cell starts to lose momentum to travel in the flow direction by friction provided by recirculating flow and bottom surface. However, other cells (*black arrow-heads*) are not trapped because they do not meet the strong recirculation. Scale bar is 100 μm. **b** By controlling the flow, a capture rate of 62% was observed for PC3 cells with less than 6% of multiple cells trapping. Scale bar is 100 μm. **c** After 2 days of culture, single or multiple cells (DsRed-transfected PC3 cells) were observed in microwells, showing the well space is large enough for cell growth and division